

compounds). In our paper, we propose structure **5** as a possible cycloenyl carbocation structure, but Haw et al.¹⁶ propose cyclopentenyl carbocation structures ($C_9H_{15}^+$, structures XIII–XIV from ref 16). In our mass spectrum, there are mass peaks with $m/e = 162$ (this peak may be assigned to structure **5** with $R_1 = H$ and $R_{2-7} = CH_3$) and with $m/e = 123$ and 122 (these peaks

may be assigned to cyclopentenyl structures XIII–XIV from ref 16) with intensities 513, 416, and 638, respectively.

Acknowledgment. We thank Dr. A. G. Pelmenchikov for helpful discussions.

Registry No. Propene, 115-07-1.

Characterization of Nylon 6 by ^{15}N Solid-State Nuclear Magnetic Resonance

Douglas G. Powell and Lon J. Mathias*

Contribution from the University of Southern Mississippi, Hattiesburg, Mississippi 39406-0076.
Received April 24, 1989

Abstract: The solid-state ^{15}N NMR characterization of nylon 6 is reported. Nylon 6 (20% ^{15}N -enriched) was prepared by anionic polymerization of isotopically enriched ϵ -caprolactam. The samples were prepared by three different treatments: quenched from the melt, slowly cooled and annealed, and artificially plasticized with excess caprolactam. CP/MAS spectra of the ^{15}N -enriched samples showed a single sharp peak (α crystal form) at 84.2 ppm (relative to glycine) and a broader resonance at 87.2 ppm. Relaxation experiments were conducted to determine T_{1N} , T_{1H} , and $T_{1\rho}$ for each sample at 300 K. The crystalline resonance was found to have T_{1N} 's of 125–416 s, consistent with crystalline nylon 6. The downfield peak had two measurable T_{1N} 's: a short component with T_{1N} of 1–3 s and a second component with a longer T_{1N} of 19–29 s. The two components for the noncrystalline peak are thought to belong to a liquidlike amorphous region and a more rigid "interphase" region lying between the crystalline and amorphous regions. $T_{1\rho N}$ measurements were consistent with two-phase (crystalline plus amorphous) morphology although the two-component decay for the amorphous region was not observed. The presence of plasticizer (caprolactam) tended to decrease $T_{1\rho N}$ relaxation times, which is consistent with lowered $T_{1\rho}$'s. 1H T_1 measurements were apparently dominated by spin diffusion that masked any differences between the regions. The chemical shift anisotropy (CSA) spectra of static samples are also shown. Motion in the amorphous region can be monitored by observing an isotropic peak at elevated temperatures. The effect of plasticizer (caprolactam) contributes to this motion. At temperatures above 100 °C, the most deshielded (σ_{33}) component is lost from the CSA spectrum, suggesting a previously unreported anisotropic motion occurring in the rigid crystalline region. This motion is thought to be associated with the intermolecular hydrogen bond between adjacent chains.

High-resolution solid-state NMR is becoming an important tool for characterizing polymer systems. Cross-polarization and magic angle spinning (CP/MAS) along with high-power decoupling allow acquisition of high-resolution spectra of natural-abundance ^{13}C nuclei with good sensitivity. The ^{13}C solid-state CP/MAS NMR of some important commercial polymers has improved our understanding of their microstructure and phase behavior.^{1–5} Relaxation studies have identified noncrystalline regions poorly characterized by X-ray.³

Recently, we have demonstrated that solid-state CP/MAS NMR of natural-abundance ^{15}N is readily obtainable on solid polyamides.^{6,7} In addition, ^{15}N CP/MAS peaks were shown to correlate with the two predominant crystal forms found in most solid polyamides, i.e., namely α and γ crystal forms. Resonances were observed for other regions that could not be assigned to either crystal form. Further study by NMR and molecular modeling calculations showed nitrogen chemical shifts to be extremely sensitive to conformation about the amide group potentially

providing a tool for observing ordered region conformations in solid polyamides.⁸

Although natural-abundance spectra are attractive from a general utility point of view, the low sensitivity of nitrogen makes observation of small amounts of impurities and reaction byproducts difficult or impossible. Relaxation experiments (T_1 , $T_{1\rho}$) are also time consuming and may be impossible on most instruments with most samples. Our interest in examining the previously unobserved noncrystalline and amorphous regions in polyamides by ^{15}N CP/MAS prompted us to prepare an isotopically enriched polyamide sample.

We chose to prepare an ^{15}N -enriched sample of nylon 6 because it is an important commercial polyamide that has been thoroughly characterized in the solid state by many techniques (DSC, IR, X-ray) including solid-state ^{13}C NMR.^{4,5} Laboratory preparation of nylon 6 is relatively straightforward. Isotopic enrichment was accomplished using commercially available hydroxylamine hydrochloride (99% ^{15}N) as shown in Figure 1. Here we report details of the polymer synthesis as well as ^{15}N NMR characterization of nylon 6 under a variety of conditions using several NMR methods.

Experimental Section

^{15}N NMR. Spectra were obtained on a Bruker MSL-200 NMR spectrometer operating at a field strength of 4.7 T and equipped with a Bruker MAS probe. The ^{15}N resonance frequency was 20.287 MHz, and that of the 1H was 200.13 MHz. Samples were placed in fused zirconia rotors fitted with Kel-F caps and spun at 3.0–3.2 kHz with dry air. Crystalline glycine was placed in the rotor with the samples and used as

(1) Veeman, W. S.; Menger, E. M.; Ritchey, W.; de Boer, E. *Macromolecules* **1979**, *12*, 924.

(2) Garroway, A. N.; Ritchey, W. M.; Moniz, W. B.; *Macromolecules* **1982**, *15*, 1051.

(3) Kitamaru, R.; Fumitaka, H.; Murayama, K. *Macromolecules* **1986**, *19*, 1943.

(4) Weeding, T. L.; Veeman, W. S.; Guar, H. A.; Huysmans, W. G. B. *Macromolecules* **1988**, *21*, 2028.

(5) Kubo, K.; Takeshi, Y.; Tadashi, K.; Ando, I.; Shiibashi, T. *J. Polym. Sci., Part B* **1989**, *27*, 929.

(6) Powell, D. G.; Sikes, A. M.; Mathias, L. J. *Macromolecules* **1988**, *21*, 1533.

(7) Mathias, L. J.; Powell, D. G.; Sikes, A. M. *Polym. Commun.* **1988**, *29*, 192.

(8) Powell, D. G.; Sikes, A. M.; Mathias, L. J. Submitted for publication.

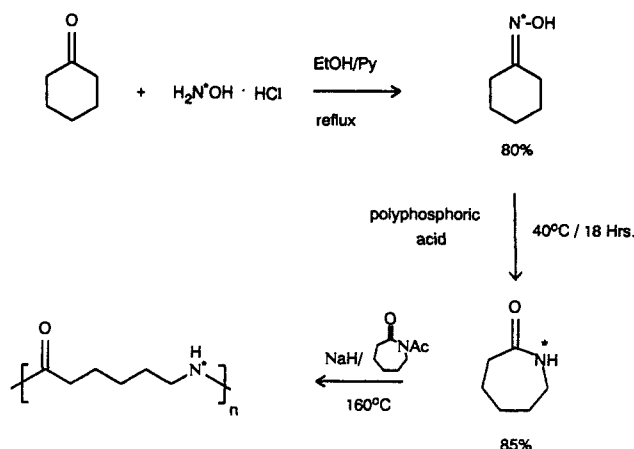


Figure 1. Reaction scheme for preparation of ^{15}N -enriched nylon 6.

an internal chemical shift reference (0 ppm). CP/MAS spectra were obtained with a standard cross-polarization pulse sequence using a 3.5- μs ^1H 90° pulse and a mixing pulse of 2 ms. High-power decoupling was used during a 50-ms acquisition time with a nutating field of 62–68 kHz. Dipolar dephasing experiments were accomplished with the pulse sequence of Opella and Frey⁹ with a delay (T_D) of 20–100 μs .

^{15}N spin-lattice relaxation times (T_{1N}) were obtained using the CP-90- τ -90 pulse sequence of Torchia.¹⁰ Other relaxation measurements were obtained using the pulse sequences shown in Figure 2. Pulse sequence I (described previously³) is a ^1H 180- τ -90 inversion-recovery experiment for measuring ^1H T_1 by monitoring the ^{15}N signal. $T_{1\rho}$ measurements were made using pulse sequence II. Pulse sequence III was used to obtain ^{15}N spectra without cross polarization.³

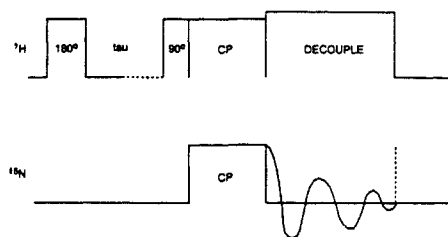
Peak deconvolution of the overlapping crystalline and amorphous resonances in the CP/MAS spectrum was accomplished using TENSOR, a Bruker-supplied Pascal program for simulating overlapping NMR resonances as combinations of Lorentzian or Gaussian line shapes. The chemical shift anisotropy of static ^{15}N spectra were simulated using POWDER, a Bruker Pascal program for simulating NMR line shapes in solids. Both programs were run on an Aspect 3000 computer.

Polymer Synthesis. Cyclohexanone and polyphosphoric acid were obtained from Aldrich Chemical Co., Milwaukee, WI. ^{15}N -labeled hydroxylamine hydrochloride (99% ^{15}N) was obtained from ICON Services, Inc., Summit, NJ. Solvents and other materials were reagent grade and used as received.

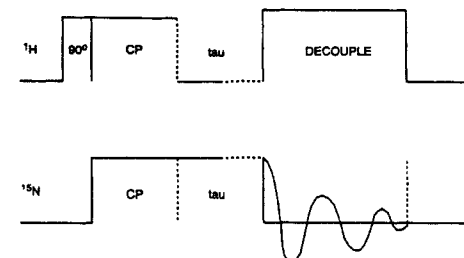
^{15}N Cyclohexanone Oxime. In a 10-mL round-bottomed flask was placed 1 g (0.014 mol) of hydroxylamine hydrochloride (99% ^{15}N) and 1.5 g (0.016 mol) of cyclohexanone. To the reactants were added 5 mL of absolute ethanol and 5 mL of dry pyridine. The flask was purged with dry nitrogen, capped with a rubber septum, and placed in an oil bath at 80 $^\circ\text{C}$ for 7 h. The solution was then poured into a 50-mL beaker, and the solvents were evaporated under a stream of dry air. The remaining amber residue was triturated with ice-cold water to precipitate the crystalline product. The crystals were filtered to yield 0.94 g (59%) of crude cyclohexanone oxime melting at 86–90 $^\circ\text{C}$. (Note: The procedure above gave the oxime in 80% yield using unlabeled hydroxylamine hydrochloride reagent. Yields of the oxime were consistently lower when using the ^{15}N -labeled hydroxylamine hydrochloride, presumably due to impurities present in the ^{15}N -labeled reagent.)

^{15}N Caprolactam. Caprolactam (99% ^{15}N) was prepared by Beckmann rearrangement of the oxime using polyphosphoric acid in a procedure similar to the one previously described.¹¹ Crude cyclohexanone oxime (400 mg) was placed in a 25-mL round-bottomed flask. Polyphosphoric acid (20 g) was added to the flask and the mixture gently heated over a low flame until the oxime dissolved. The flask was capped with a rubber septum and placed in an oil bath at 50–55 $^\circ\text{C}$ for 18 h. The flask was removed from the bath, and 10 mL of ice-cold water was added with stirring. The aqueous mixture was poured into a 150-mL beaker and 2 or 3 drops of phenolphthalein indicator solution added. The acidic solution was titrated with 4 N KOH until basic. The slightly basic solution was extracted with four 50-mL portions of dichloromethane. The organic layers were combined, and the dichloromethane was evaporated in a stream of air to yield a white crystalline solid. The product was further purified by column chromatography (150-mesh basic alumina with a mobile phase of 5% (v/v) $\text{MeOH}/\text{CH}_2\text{Cl}_2$) to remove phe-

I. ^1H T_1



II. $T_{1\rho N}$



III. ^{15}N (without CP)

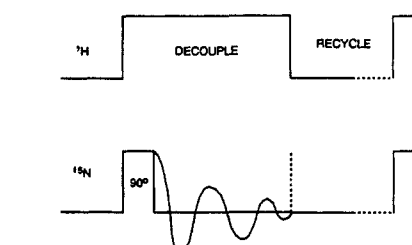


Figure 2. Pulse sequences used in this paper.

nolphthalein. After evaporation of the solvents, the product was recrystallized from hot cyclohexane to give [^{15}N] caprolactam: mp 69–70 $^\circ\text{C}$; yield 350 mg (85%). The purified ^{15}N -labeled caprolactam was combined with unlabeled material to give approximately 20% ^{15}N content. This material was used for polymerization reactions described below.

^{15}N Nylon 6. Caprolactam (250 mg at 20% ^{15}N enrichment) was weighed into an oven-dried glass vial. To this was added 3 μL of *N*-acetylcaprolactam. The vial was placed in an oil bath at 160 $^\circ\text{C}$ and purged with a slow stream of dry nitrogen. Sodium hydride (10 mg of a 60% dispersion in mineral oil) was added all at once to the molten solution. After about 30 s, the solution became opaque and viscous. The polymerization was continued for 5 min. The vial was then removed from the bath and allowed to cool. The vial was crushed, and the solid nylon plug was recovered in quantitative yield. A portion of the crude in situ reaction product was retained for further study. The remainder was extracted overnight with methanol and dried under vacuum at 80 $^\circ\text{C}$.

The extracted samples were placed between sheets of aluminum foil coated with a fluoropolymer mold release agent and then melt-pressed at 250 $^\circ\text{C}$ (20 ksi) to give films of approximately 0.3-mm thickness. The molten samples were either quenched in ice-cold water or annealed in the press at 160 $^\circ\text{C}$ for 2 h. The percent crystallinity was determined by DSC measurement of the heat of fusion for each sample as previously described.¹²

Results and Discussion

1. CP/MAS and T_{1N} of Crystalline and Amorphous Nylon 6. The CP/MAS spectrum of nylon 6 is shown in Figure 3. Only 18 000 scans were required to obtain excellent signal to noise for this 100-mg sample. The spectrum shown is similar to natural-abundance ^{15}N spectra we previously reported.^{6,7} The main strong peak clearly overlaps a broader resonance at lower field. The overlapping peaks were fit with a composite line shape (Figure 3, lower trace) and the individual components deconvoluted as shown. From the deconvoluted components, the upfield resonance is located at 84.2 ppm with a line width at half-height of 2.4 ppm. This peak was previously correlated with the α crystal form of nylon 6.^{6,7} The broader downfield resonance is centered at 87.2

(9) Opella, S. J.; Frey, M. H. *J. Am. Chem. Soc.* **1979**, *101*, 5856.

(10) Torchia, D. A. *J. Magn. Reson.* **1978**, *30*, 613.

(11) Pearson, D. E.; Stone, R. M. *J. Am. Chem. Soc.* **1961**, *83*, 1715.

(12) Inoue, M. *J. Polym. Sci., Part A* **1963**, *1*, 2697.

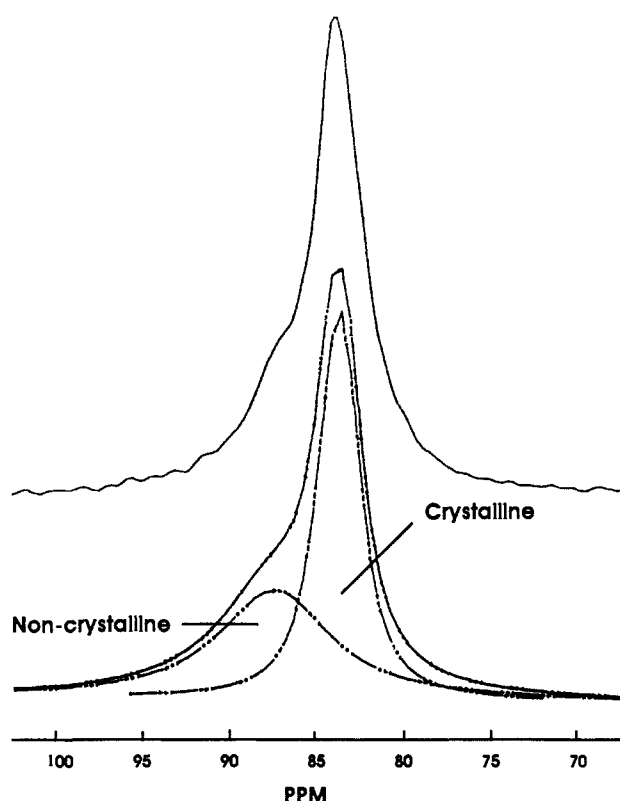


Figure 3. (Upper trace, 18 000 FID's) ^{15}N CP/MAS spectrum of ^{15}N -enriched nylon 6 showing α crystal form (large peak at approximately 84 ppm) and broader, overlapping region downfield (noncrystalline region). (Lower trace) TENSOR fit of the ^{15}N CP/MAS line shape of nylon 6 along with the individual components.

ppm and possesses a line width at half-height of 6.3 ppm. This resonance had not been observed in our previous work with polyamides at the ^{15}N natural-abundance level. We believe this to be the signal from the noncrystalline or "amorphous" fraction of the nylon sample since its chemical shift appears midway between the α and γ resonances typically observed for nylon 6⁶ and other nylons.⁷ (The γ form gives a sharp resonance at 88.5 ppm.)⁶

To conclusively identify the downfield resonance as that of the amorphous region, relaxation experiments were conducted to evaluate the mobility of each region by monitoring spin-lattice relaxation times ($T_{1\text{N}}$). Using the method of Torchia,¹⁰ relaxation times $T_{1\text{N}}$ were obtained at 300 K for resonances at 84.2 ppm (α crystal resonance) and 87.2 ppm (approximate position of the amorphous resonance) for several samples. Figure 4 displays the ^{15}N spectra obtained with τ delays shown. The downfield amorphous resonance decays rapidly while the crystalline peak at 84.2 ppm remains strong after 40 s. Peak intensities I were plotted vs τ and the data fitted to an exponential function: $I = I_0 e^{-\tau/T}$ where I_0 is the intensity at $\tau = 0$ and T is the spin-lattice relaxation time ($T_{1\text{N}}$). Figure 5 shows a plot of magnetization decay for the crystalline component of the annealed sample. The crystalline component had a $T_{1\text{N}}$ of 416 s. Figure 6 shows the two-component decay of the amorphous fraction of the same sample with a $T_{1\text{N}}$ of 29.1 s and an additional component with $T_{1\text{N}}$ of 1.9 s. The two shorter $T_{1\text{N}}$'s for the 87.2 ppm are consistent with an amorphous fraction with much greater mobility than the crystalline portion of the sample. In addition, the detection of two $T_{1\text{N}}$'s may indicate two types of amorphous regions: a bulk amorphous fraction with liquidlike mobility and a noncrystalline "interphase" region with restricted motion. Similar phase morphology is observed in polyethylene where the crystalline and the noncrystalline interphase regions are clearly delineated by their $T_{1\text{C}}$ relaxation times.³ To our knowledge, this is the first report of NMR observation of an interphase region in a semicrystalline polyamide as well as the first relaxation measurements of crystalline and amorphous regions by ^{15}N CP/MAS.

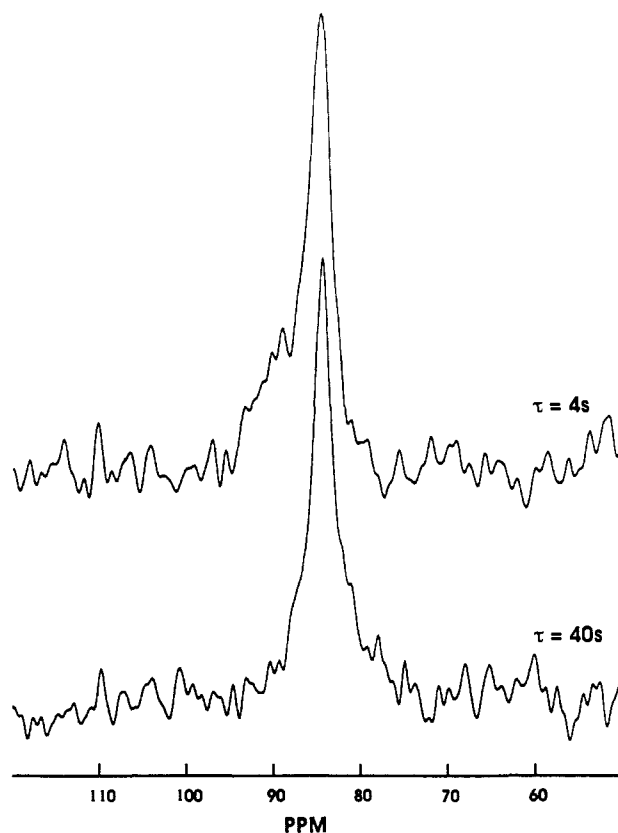


Figure 4. ^{15}N spectra obtained from the CPT_1 pulse sequence of Torchia with τ delays shown. The lower trace ($\tau = 40$ s) shows mainly the crystalline component with long $T_{1\text{N}}$.

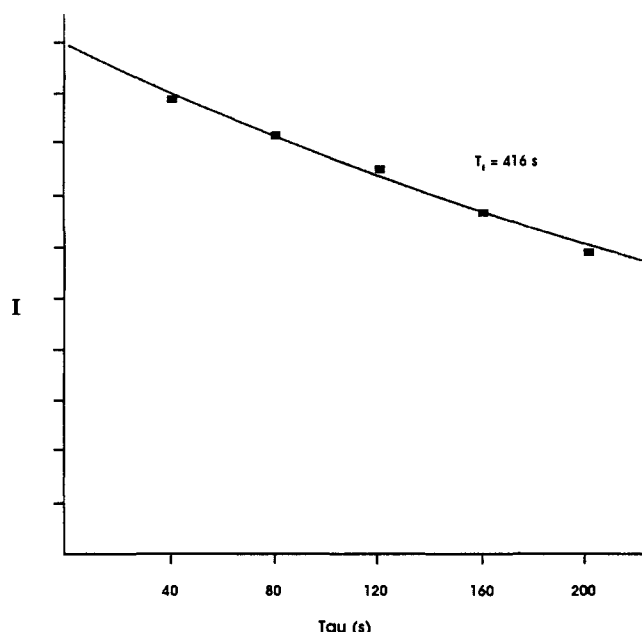


Figure 5. ^{15}N spin-lattice relaxation of nylon 6. Plot of intensity of ^{15}N resonance at 84.2 ppm versus τ along with single-exponential fit used to determine $T_{1\text{N}}$.

^{15}N T_1 measurements are also reported in Table I for the in situ prepared sample as well as extracted samples that were quenched from the melt. The amorphous regions in all samples have shorter relaxation times than the crystalline regions, a fact consistent with ^{13}C relaxation studies of these materials.⁴ In addition, the in situ prepared samples have shorter $T_{1\text{N}}$ values than any of the methanol-extracted samples. Since the $T_{1\text{N}}$ values are associated with motions of the polymers, a shorter $T_{1\text{N}}$ value for the in situ sample indicates more rapid motion, due either to plasticization by residual caprolactam in the sample or differences

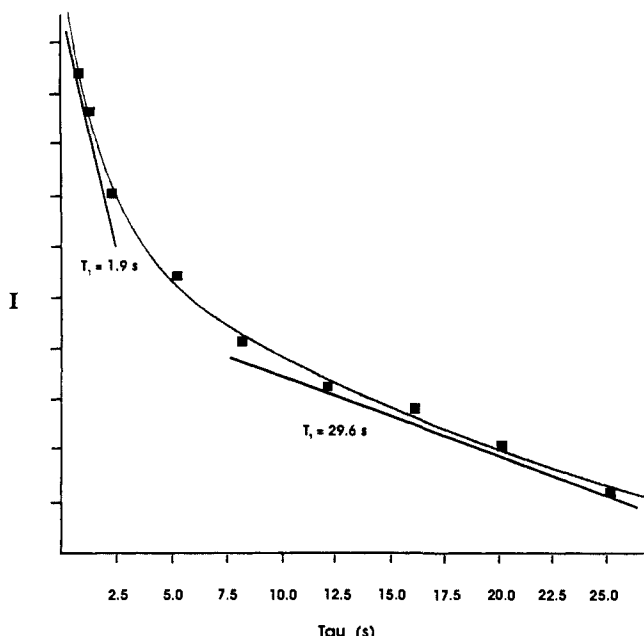


Figure 6. ^{15}N spin-lattice relaxation of nylon 6. Plot of intensity of ^{15}N resonance at 87.2 ppm versus τ . The biexponential fit is plotted along with individual $T_{1\text{N}}$ components showing two-component decay.

Table I

sample	% xtal	param	amorphous phase (87.2 ppm)	crystalline phase (84.2 ppm)
in situ	23	$T_{1\text{N}}$	a, 26 s	111.5 s
		$T_{1\text{H}}$	0.99 s	0.95 s
		$T_{1\rho}$	b	13.8 ms
melt quenched	29	$T_{1\text{N}}$	2.7 s, 19 s	230 s
		$T_{1\text{H}}$	1.06 s	1.03 s
		$T_{1\rho}$	24.3 ms	44.5 ms
annealed (160 °C)	45	$T_{1\text{N}}$	1.9 s, 29.1 s	416 s
		$T_{1\text{H}}$	0.75 s	0.78 s
		$T_{1\rho}$	37.9 ms	57.7 ms

^aShort T_1 component was not observed for this sample. ^bDecayed too rapidly to be observed.

in the crystalline regions. Caprolactam has been shown to plasticize polyamides to improve flexibility and elongation.^{13,14} Increased motion brought about by plasticization may account for the difference in relaxation times $T_{1\text{N}}$ for the amorphous region. The increase in $T_{1\text{N}}$ for the crystalline region of the unplasticized samples cannot be attributed to plasticizer effects. However, the process of extraction and heating of the sample may alter the size of crystalline domains. Spin-lattice relaxation times of semi-crystalline polymers have been shown to increase substantially with increasing crystal lamellar thickness.¹⁵ The increase in $T_{1\text{N}}$ on annealing the sample is consistent with increasing crystal lamellae thickness.

We took advantage of the difference in spin-lattice relaxation times $T_{1\text{N}}$ between the two phases to directly observe the amorphous fraction. Using pulse sequence III shown in Figure 2, a MAS spectrum of the ^{15}N -labeled nylon 6 was obtained without cross polarization. By using a recycle delay of 5–10 s, the ^{15}N magnetization in the rigid, crystalline regions is quickly saturated. The nuclei in the amorphous region with shorter $T_{1\text{N}}$ can then be observed directly. When this method was used, the spectrum of the amorphous region was obtained (Figure 7, lower trace). This spectrum is nearly identical with the deconvoluted peak from the CP/MAS spectrum shown in Figure 3; i.e., the

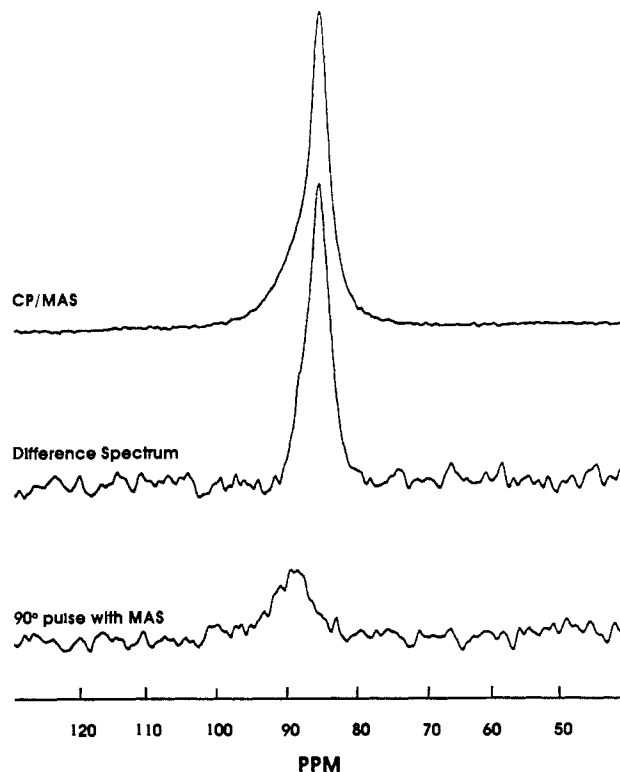


Figure 7. ^{15}N MAS spectra of nylon 6 at 300 K. (Upper trace) Spectrum with cross polarization; main peak for α crystal form is seen along with overlapping resonance downfield. (Lower trace) ^{15}N spectrum obtained using pulse sequence III (recycle delay of 5 s) showing only the noncrystalline region with shorter $T_{1\text{N}}$. (Center trace) Spectral subtraction of upper and lower traces showing the symmetrical resonance line for the α crystal form of nylon 6.

resonance is broad and downfield of the α crystal peak but upfield from the observed position of the γ crystal peak. Spectral subtraction gives the center trace in Figure 7. Now the resonance for the α crystal form is clearly seen as a symmetrical Lorentzian line, with contributions from the noncrystalline region removed.

2. Static Cross-Polarization Spectra (Chemical Shift Anisotropy). The anisotropic chemical shifts (CSA) in solids can yield much information about the local electronic environment of a nucleus.¹⁶ Although tensor elements have been estimated from the powder spectra of a number of ^{15}N -containing compounds,^{17,18} only one single-crystal ^{15}N study has been reported for an amide (glycylglycine) giving tensor orientations with respect to bond angles.¹⁹ We are aware of no previous reports in the literature describing ^{15}N chemical shift anisotropies of polyamides. This is not surprising since the random orientations of nuclei in semi-crystalline polymers precludes absolute determination of tensor orientations with respect to the bond direction. Nevertheless, ^{13}C CSA spectra of polymers can be sensitive to motions in the solid state.²⁰ ^{15}N CSA spectra should be superior to ^{13}C for probing nylon 6 since only one chemically distinct nitrogen is present in the polyamide repeat unit.

A static ^{15}N CP spectrum of nylon 6, which had been extracted with methanol, is shown in Figure 8, lower trace. The upper trace in Figure 8 shows the calculated CSA powder spectrum at 300 K. From POWDER calculations the individual tensors of the an-

(13) Saito, H.; Murakami, T. *Jpn. Patent* 62/41315; *Chem. Abstr.* **1987**, *107*, 98119.

(14) Cogswell, F. N.; Nield, E.; Staniland, P. A. *Eur. Patent* 102158; *Chem. Abstr.* **1984**, *100*, 211109.

(15) Axelson, D. E.; Mandelkern, L.; Popli, R.; Mathieu, P. J. *Polym. Sci., Polym., Phys. Ed.* **1983**, *21*, 2319.

(16) Fyfe, C. A. *Solid State NMR for Chemists*; C. F. C. Press: Guelph, Ontario, Canada, 1983; pp 201–2.

(17) Valentine, K. G.; Rockwell, A. L.; Gierasch, M.; Opella, S. J. *J. Magn. Reson.* **1987**, *73*, 519.

(18) Oas, T. G.; Hartzell, C. J.; Dahlquist, F. W.; Drobny, G. P. *J. Am. Chem. Soc.* **1987**, *109*, 5962.

(19) Harbison, G. S.; Jelinski, L. W.; Stark, R. E.; Torchia, D. A.; Herzfeld, J.; Griffin, R. G. *J. Magn. Reson.* **1984**, *60*, 79.

(20) Jones, A. A. In *High Resolution NMR Spectroscopy of Synthetic Polymers in Bulk*; Komoroski, R. A., Ed.; VCH Publishers, Inc.: Deerfield Beach, FL, 1986; pp 261–74.

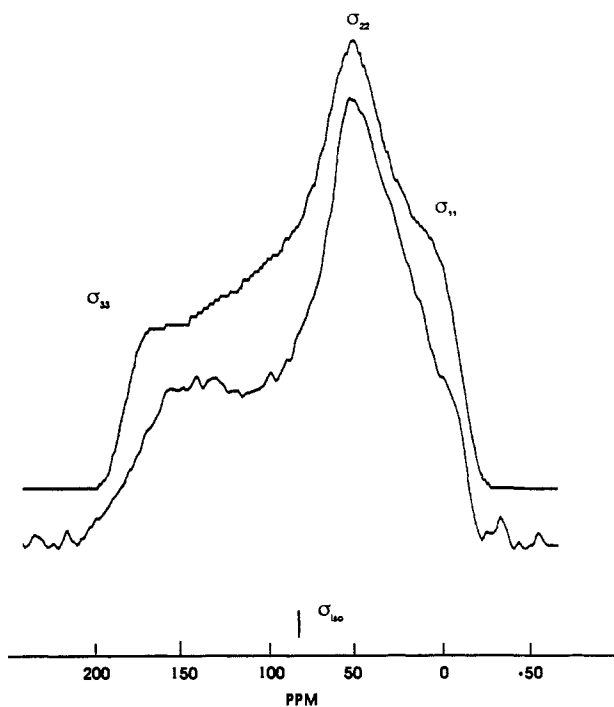


Figure 8. Static ^{15}N CSA spectrum of methanol-extracted sample at 300 K. Upper trace is the best fit from POWDER showing the relative positions of the tensor components.

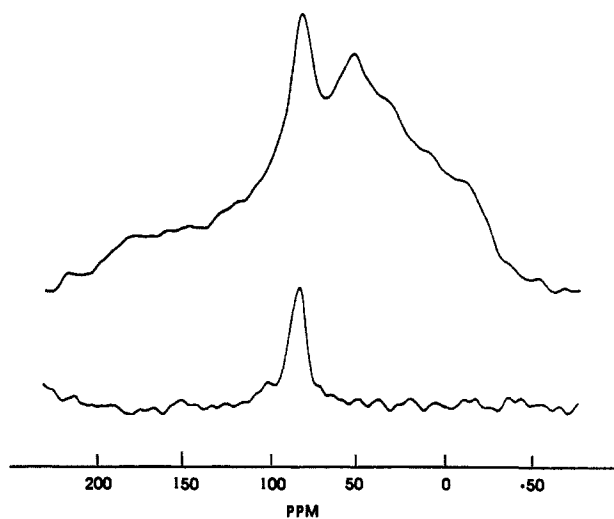


Figure 9. Static ^{15}N NMR CSA spectrum of in situ prepared nylon 6 at 350 K. (Top trace) CP spectrum showing both crystalline and non-crystalline components. (Bottom trace) Spectrum obtained with a 90° pulse and decoupling (recycle delay of 7 s) showing noncrystalline components.

isotropy were calculated: $\sigma_{11} = 5$ ppm; $\sigma_{22} = 60$ ppm; $\sigma_{33} = 180$ ppm. The calculated isotropic chemical shift (σ_{iso}) is 81.6 ppm, in good agreement with the value of 84.2 ppm obtained through MAS.

The pattern shown in Figure 9, upper trace, is the in situ prepared sample at 350 K, i.e., slightly above T_g . A peak with narrow line width is seen at approximately 84 ppm while the remainder of the spectrum is a typical pattern for a nonaxial shielding tensor. The upper trace was obtained using the normal CP pulse sequence. The lower trace was obtained without CP by using pulse sequence III and a recycle delay of 7 s. The rigid, crystalline components with long $T_{1\text{N}}$ have become saturated in the lower spectrum with the resonance for the mobile fraction remaining. It was thought that the peak in the lower spectrum might be the result of plasticization of the noncrystalline component by ^{15}N -labeled caprolactam still dissolved in the sample (which should be a liquid at this temperature). Plasticization was

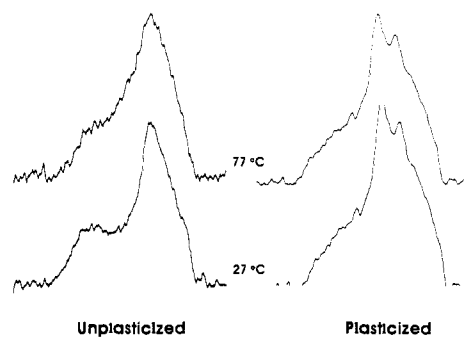


Figure 10. ^{15}N CSA powder spectra of nylon 6. (Left column) Methanol-extracted samples (unplasticized) by caprolactam. (Right column) Samples plasticized by heating in molten caprolactam.

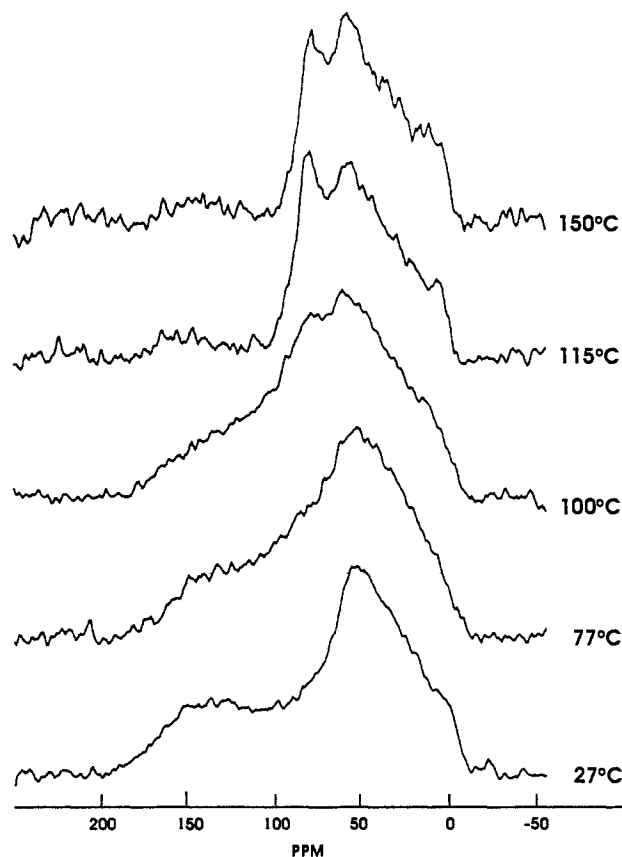


Figure 11. Static ^{15}N NMR spectrum of annealed nylon 6 sample obtained with cross polarization and high-power decoupling at different temperatures. The noncrystalline component at approximately 84 ppm becomes increasingly sharper at elevated temperatures.

confirmed by taking the extracted nylon 6 and immersing it in molten (unlabeled) caprolactam at 120°C . Figure 10 shows the CSA spectra of plasticized and unplasticized nylon 6 at two different temperatures. It can be seen that the isotropic resonance is more intense for the plasticized sample at a given temperature. The narrowing of the isotropic peak on addition of plasticizer gives clear evidence that plasticization is increasing the motional freedom of the amorphous fraction. The powder pattern for the crystalline fraction remains virtually unchanged at these temperatures.

Cross-polarization ^{15}N CSA spectra of the extracted (unplasticized) sample were obtained for a series of temperatures as shown in Figure 11. At 27°C , the nonaxial powder pattern is seen. As the temperature is increased, a narrow amorphous resonance appears centered near 84 ppm. This peak becomes more intense at higher temperatures and is clearly seen above 100°C . The chemical shift of the amorphous fraction (84.3 ppm) approaches the isotropic chemical shift obtained with MAS. Again, rapid motion has averaged the anisotropy of the amorphous fraction. However, higher temperatures are required to achieve

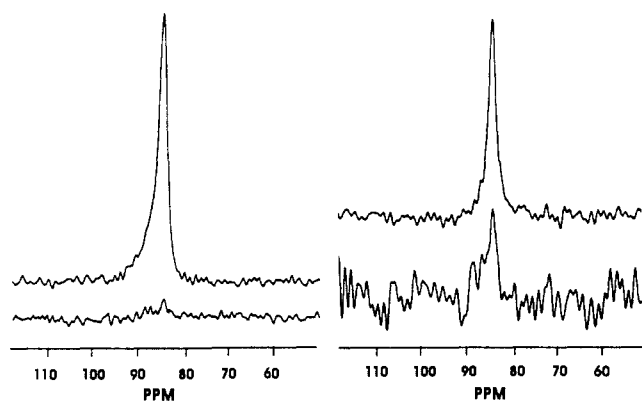


Figure 12. ^{15}N dipolar dephasing spectrum of methanol-extracted nylon 6 at 300 K (left) and at 370 K (right). In the upper trace in each experiment ($T_D = 20 \mu\text{s}$), the magnetization remains intact. (Lower trace, left) $T_D = 100 \mu\text{s}$ with rigid components dephased. (Lower trace, right) At 370 K, the resonance at 84 ppm (a crystal resonance) is not completely dephased ($T_D = 120 \mu\text{s}$) indicating onset of rapid motion in the crystalline region.

the same motion that is observed in the plasticized nylon sample.

Another interesting phenomenon is observed in the CSA spectra of Figure 11. As the temperature is increased from 27 to 100 °C, the downfield component of the powder pattern (σ_{33}) becomes smaller. At 115 °C this component is either no longer sharply defined or has disappeared altogether. Note also that the σ_{22} and σ_{11} elements remain essentially unchanged from the room-temperature spectrum. This indicates a retention of nonaxial symmetry since, in an axially symmetric pattern, the σ_{22} and σ_{11} elements should average to some intermediate value.¹⁶ Although the pattern remains nonaxially symmetric, the loss of the σ_{33} component at elevated temperature suggests the onset of anisotropic motion associated with this tensor component.

One possible explanation is that a change or transition in intermolecular hydrogen bonding at elevated temperatures occurs that apparently does not destroy the crystal structure. Interestingly, the tensor element σ_{33} associated with this component has been shown to lie nearly parallel to the NH bond in amides.¹⁹ An infrared study of the effect of temperature on hydrogen bonding in amorphous nylons by Skrovanek and co-workers²¹ found that the amide groups remain nearly 100% hydrogen bonded at temperatures up to the melting point. Frequency shifts and changes in absorptivity in the IR were attributed to relatively large vibrational displacements of the NH bond.²¹ In the crystalline region of the polyamide, the relatively small hydrogen will have the best chance for rapid motion even in the solid lattice. Another possible explanation is that a change in cross-polarization efficiency may be occurring which affects only the intensity of σ_{33} in the spectrum. The relatively constant chemical shift of the highly mobile, noncrystalline resonance also argues against a true "loss" of σ_{33} . Nevertheless, it appears likely that, by whatever mechanism, anisotropic motion or libration in the crystalline region is responsible for the phenomenon observed here.

This argument is further supported by dipolar dephasing experiments (Figure 12) on the methanol-extracted nylon 6 samples at 300 K (left) and 350 K (right). By turning off the decoupler for a delay T_D , dipolar interactions between ^{15}N and ^1H cause the signal to decay. Rapidly moving regions of the sample, however, do not dephase completely. Any residual signal indicates motion is occurring that serves to prevent complete dephasing. The upper trace in each experiment shows the normal CP/MAS result. The lower trace shows the dephased spectrum. At 300 K, (Figure 12, lower left) the rigid, crystalline resonance decays into the base-line noise.

At 370 K (upper limit for MAS with our probe) the experiment (Figure 12, lower right) shows a small resonance remaining at T_D of 120 μs . At this temperature, enough motion is present to

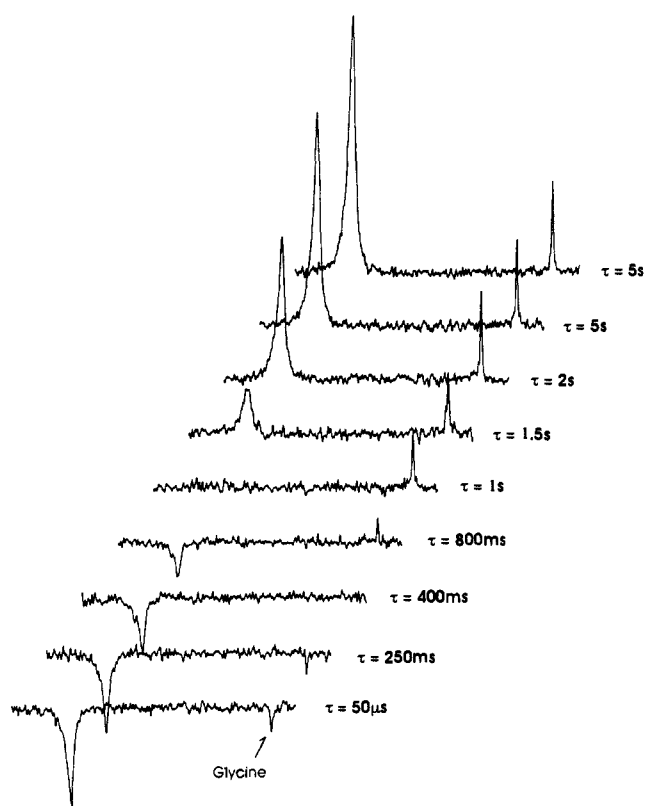


Figure 13. Stack plot of ^{15}N CP/MAS spectra obtained with pulse sequence I using τ delays shown. The trace with $\tau = 1 \text{ s}$ shows equivalent inversion of crystalline and amorphous ^{15}N resonances, an indication that both the crystalline and amorphous regions have equivalent $T_{1\text{H}}$ due to rapid spin diffusion between phases.

weaken the dipolar interaction such that the signal is not completely lost. This peak at approximately 84 ppm is correlated with the resonance for the α crystal form, supporting our CSA observations that significant motion is occurring in the crystalline region of the sample.

3. $T_{1\text{H}}$ and Spin Diffusion. $T_{1\text{H}}$ measurements were made using pulse sequence I at temperatures of 300 and 350 K. The $T_{1\text{H}}$ values were obtained by measuring the recovery of the ^{15}N magnetization at different τ . Since the ^{15}N resonances were already determined for the crystalline and amorphous components, the proton relaxation of each phase can be measured by observing the decay of the ^{15}N magnetization as shown in Figure 13. The $T_{1\text{H}}$ values of the in situ sample and the extracted sample are shown in Table I.

The ^1H T_1 values for each sample are about 1 s, very close to those for the crystalline region of polyethylene.³ Unlike polyethylene, which contains a very liquidlike amorphous region³ with a much shorter $T_{1\text{H}}$, the amorphous region of nylon 6 has very nearly the same $T_{1\text{H}}$. The fact that the two phases have very different $T_{1\text{N}}$ but similar $T_{1\text{H}}$ indicates rapid ^1H spin diffusion between the phases. To confirm that the fast ^1H spin diffusion observed was not unique to the ^{15}N nucleus, the analogous relaxation experiment observing the ^{13}C nucleus was performed. ^{13}C resonances for the crystalline and amorphous regions (previously identified by Veeman⁴) were measured. The nearly identical $T_{1\text{H}}$ values obtained here confirm rapid spin diffusion between the crystalline and noncrystalline phases.

4. $T_{1\rho}$ Measurements. $T_{1\rho\text{N}}$ measurements were made using pulse sequence II and are reported in Table I. The crystalline region has the longer relaxation time (13–58 ms) and the amorphous region the shorter (0–40 ms). Although the increase in relaxation times $T_{1\rho\text{N}}$ correlates with increasing percent crystallinity, the large differences in relaxation times seen for ^{15}N T_1 are not evident. The reason for this has been discussed by several authors studying semicrystalline polymers by ^{13}C CP/MAS.^{22–24} They point out that rotating-frame relaxation ($T_{1\rho}$)

(21) Skrovanek, D. J.; Howe, S. E.; Painter, P. C.; Coleman, M. M. *Macromolecules* **1985**, *18*, 1676.

is not pure spin-lattice in nature but has a considerable spin-spin (T_2) component due to rapid ^1H spin diffusion between the different phases.²³ In highly crystalline systems, the rotating-frame relaxation $T_{1\rho}$ was found to be completely dominated by spin-spin relaxation.²⁴ In such systems, the $T_{1\rho}$ of the crystalline phase is usually shorter than the amorphous region because of more efficient T_2 in the crystalline region. In these nylon 6 samples, however, the $T_{1\rho\text{N}}$ values mimic the $T_{1\text{N}}$ data. Spin diffusion, although highly evident in the nearly identical $T_{1\text{H}}$ values for both the crystalline and amorphous phases, does not dominate $T_{1\rho\text{N}}$. Nevertheless, the two amorphous components seen in the $T_{1\text{N}}$ relaxation experiment are not evident from $T_{1\rho\text{N}}$ measurements. Similar to the $T_{1\text{N}}$ data, the increase in $T_{1\rho\text{N}}$ of the crystalline component may be related to changing crystallite size.

Conclusions

The ^{15}N -labeled nylon 6 sample was prepared in good yield by anionic polymerization of the ^{15}N -labeled ϵ -caprolactam monomer. Enrichment of approximately 20% ^{15}N has allowed direct $T_{1\text{N}}$ and $T_{1\rho\text{N}}$ relaxation measurements as well as $T_{1\text{H}}$ determination by indirect observation of ^{15}N cross polarization.

As expected, the rigid crystalline region has a much longer $T_{1\text{N}}$ relaxation than the more mobile amorphous region. The $T_{1\text{N}}$ of the crystalline fraction was 111-416 s. Two components were observed in the relaxation of the amorphous peak: a fast component with T_1 of 1-3 s and a longer component with T_1 of 19-29 s. The two noncrystalline components are thought to belong to

amorphous and noncrystalline interphase regions, respectively.

Less dramatic behavior is seen in $T_{1\rho\text{N}}$ relaxation times. Only a single amorphous component could be observed. This anomaly is attributed to considerable ^1H spin-spin relaxation within the sample resulting in similar $T_{1\rho\text{N}}$ values. This conclusion is further supported by ^1H T_1 relaxation experiments, which show that rapid ^1H spin diffusion is occurring between the phases. Addition of plasticizers, which concentrate in the amorphous region, apparently decreases the observed $T_{1\rho\text{N}}$ of both the crystalline and amorphous regions. However, the effect on the crystalline $T_{1\rho\text{N}}$ may be better attributed to differences in crystallite size than to increased motion.

The first chemical shift anisotropy patterns of a polyamide have been obtained on nylon 6. The CSA powder patterns show the growth of an amorphous signal at elevated temperatures with a chemical shift near the isotropic value obtained with MAS. The addition of plasticizer (caprolactam) causes this signal to grow in at lower temperatures, confirming that plasticization is increasing molecular mobility in the amorphous region. The σ_{33} component becomes less prominent with increasing temperature and finally disappears above 115 °C. The phenomenon has not been previously reported but is postulated to be the result of anisotropic motion associated with the tensor component σ_{33} , which lies along the NH bond of the amide group.

Acknowledgment. We gratefully acknowledge a Department of Defense instrumentation grant with which we purchased our Bruker MSL-200 spectrometer. This research was supported in part by a grant from the Office of Naval Research. We also thank Dr. William L. Jarrett for helpful discussions concerning the NMR pulse experiments reported here.

Registry No. Nylon 6, 25038-54-4; ϵ -caprolactam, 105-60-2.

(22) Menger, E. M.; Veeman, W. S.; de Boer, E. *Macromolecules* **1982**, *15*, 1406.

(23) Veeman, W. S.; Menger, E. M. *Bull. Magn. Reson.* **1980**, *2*, 77.

(24) VanderHart, D. L.; Garroway, A. N. *J. Chem. Phys.* **1979**, *71*, 2773.

A Quantitative Clarification of Vibrationally Coupled Dioxygen in the Resonance Raman Spectra of Cobalt-Substituted Heme Proteins and Model Compounds

Leonard M. Proniewicz¹ and James R. Kincaid*

Contribution from the Chemistry Department, Marquette University, Milwaukee, Wisconsin 53233. Received April 24, 1989

Abstract: The resonance Raman (RR) spectra of dioxygen adducts of cobalt porphyrin complexes with various trans-axial bases and cobalt-substituted heme proteins exhibit complicated spectral patterns characterized by the appearance of weak secondary features and unexpected frequencies and intensities of the $\nu(\text{O}-\text{O})$ of the various dioxygen isotopomers. These patterns are shown to derive from vibrational resonance coupling of $\nu(\text{O}-\text{O})$ with internal modes of the trans-axial ligand. The observed frequency perturbations and intensities agree, within experimental error, with those calculated by using the conventional Fermi resonance coupling scheme. Further, it is shown that a careful quantitative treatment of spectral data for the proteins provides accurate estimates of the frequencies of particular modes associated with the coordinated histidylimidazole fragment.

Vibrational spectroscopy has long served as a powerful probe of the structure and bonding of dioxygen adducts of metal complexes.^{2,3} It is therefore not surprising that much effort has been devoted to its utilization for the study of the O_2 adducts of nature's oxygen transport proteins, hemoglobin (Hb) and myoglobin (Mb), inasmuch as it potentially provides a relatively convenient and sensitive method to directly monitor even subtle changes in structure and bonding of the metal-oxygen linkage. While some important new information has been gained from both infrared⁴

and resonance Raman spectroscopies,^{5,6} several problems have prevented these techniques from providing information at a level of sophistication which is commensurate with their inherent promise.

The problems encountered for IR studies essentially arise from the experimental difficulties associated with extracting the $\nu(\text{O}-\text{O})$ and $\nu(\text{M}-\text{O})$ absorptions from those due to the protein matrix.⁴

(4) Caughey, W. S. In *Methods for Determining Metal Ion Environments in Proteins: Structure and Function of Metalloproteins*; Darnall, D. W.; Wilkins, R. G., Eds.; Elsevier: North Holland, New York, 1980; p 95.

(5) Spiro, T. G. In *Iron Porphyrins*; Lever, A. B. P., Gray, H. B., Eds.; Addison-Wesley Publishing Co.: Reading, MA, 1983; Part II, p 89.

(6) Yu, N.-T., Kerr, E. A. In *Biological Applications of Raman Spectroscopy*; Spiro, T. G., Ed.; Wiley-Interscience: New York, 1987; Vol. 3, p 39.

(1) Permanent address: Regional Laboratory of Physicochemical Analyses and Structural Research, Jagiellonian University, Cracow, Poland.

(2) Nakamoto, K. *Infrared and Raman Spectra of Inorganic and Coordination Compounds*; Wiley-Interscience: New York, 1986; p 414.

(3) Nakamoto, K. *Coord. Chem. Rev.*, in press.